Conformational Behavior and Aggregation of α-Synuclein in Organic Solvents: Modeling the Effects of Membranes[†]

Larissa A. Munishkina,[‡] Cassandra Phelan,[‡] Vladimir N. Uversky,*[,‡,§] and Anthony L. Fink*[,‡]

Department of Chemistry and Biochemistry, University of California, Santa Cruz, California 95064, and Institute for Biological Instrumentation, Russian Academy of Sciences, Pushchino, Moscow Region 142292, Russia

Received November 12, 2002; Revised Manuscript Received December 20, 2002

ABSTRACT: Intracellular proteinaceous inclusions (Lewy bodies and Lewy neurites) of α-synuclein are pathological hallmarks of neurodegenerative diseases such as Parkinson's disease, dementia with Lewy bodies (DLB), and multiple systemic atrophy. The molecular mechanisms underlying the aggregation of α-synuclein into such filamentous inclusions remain unknown, although many factors have been implicated, including interactions with lipid membranes. To model the effects of membrane fields on α-synuclein, we analyzed the structural and fibrillation properties of this protein in mixtures of water with simple and fluorinated alcohols. All solvents that were studied induced folding of α-synuclein, with the common first stage being formation of a partially folded intermediate with an enhanced propensity to fibrillate. Protein fibrillation was completely inhibited due to formation of *β*-structure-enriched oligomers with high concentrations of methanol, ethanol, and propanol and moderate concentrations of trifluoroethanol (TFE), or because of the appearance of a highly α-helical conformation at high TFE and hexafluoro-2-propanol concentrations. At least to some extent, these conformational effects mimic those observed in the presence of phospholipid vesicles, and can explain some of the observed effects of membranes on α-synuclein fibrillation.

Parkinson's disease (PD)[1] is the second most common neurodegenerative disorder, after Alzheimer's disease, and affects >1% of the U.S. population over the age of 60. Clinically, PD is a movement disorder, due to the progressive loss of dopaminergic neurons from the *substantia nigra*. Some surviving nigral dopaminergic neurons contain cytosolic filamentous inclusions known as Lewy bodies and Lewy neurites (*1*, *2*). LBs and LNs also are also found in other brain regions and several other neurodegenerative disorders (*2*−*6*). The basis for the degeneration of dopaminergic neurons in PD patients is still unknown. However, several observations lead to the conclusion that aggregation of the presynaptic protein α-synuclein is involved in the pathogenesis of PD. α-Synuclein was shown to be a major fibrillar component of LBs and LNs (*7*, *8*). Two different missense mutations in the α-synuclein gene, corresponding to A53T and A30P substitutions in α-synuclein, have been identified in two or three kindreds with autosomal-dominantly inherited, early-onset PD (*9*, *10*). Furthermore, the production of WT α-synuclein in transgenic mice (*11*) or of the wild type, A30P, and A53T in transgenic flies (*12*) leads to the motor deficits and neuronal inclusions reminiscent of PD. These observations indicate that α-synuclein is a key player in the pathogenesis of several neurodegenerative disorders.

α-Synuclein is a small (14 kDa), soluble, intracellular, highly conserved protein, of unknown function, that is abundant in various regions of the brain (*13*−*16*), and has been estimated to account for as much as 1% of the total protein in soluble cytosolic brain fractions (*15*). It is characterized by the presence of acidic stretches within the C-terminal region and a repetitive motif, KTKEGV, in the first 93 residues (*16*, *17*). Such a periodicity is characteristic of the amphipathic helices of apolipoproteins (*16*, *18*, *19*) and provides α-synuclein with a class A2 lipid-binding helix motif, distinguished by the clustered basic residues at the polar−apolar interface, positioned ±100° from the center of the apolar face; a predominance of lysines relative to arginines among these basic residues; and several glutamate residues at the polar surface (*19*−*21*). In accord with these structural features, α-synuclein has been shown to bind specifically to natural and synthetic vesicles (*20*−*28*).

Structurally, purified α-synuclein is a natively unfolded protein (*29*−*31*). This lack of folded structure has been shown to correlate with specific combinations of low overall hydrophobicity and large net charge (*32*−*34*). The functional importance of being disordered has been analyzed (*35*−*42*), and it has been proposed that the increased intrinsic plasticity represents an important prerequisite for effective molecular

[†] This research was supported by Grant RO1 NS39985 from the National Institutes of Health.

* To whom correspondence should be addressed: Department of Chemistry and Biochemistry, University of California, Santa Cruz, CA 95064. Telephone: (831) 459-2744. Fax: (831) 459-2935. E-mail: fink@chemistry.ucsc.edu or uversky@hydrogen.ucsc.edu.

[‡] University of California.

[§] Russian Academy of Sciences.

[1] Abbreviations: PD, Parkinson's disease; AD, Alzheimer's disease; LB, Lewy bodies; LN, Lewy neurites; DLB, dementia with LB; LBVAD, LB variant of AD; WT, wild type; NAC, non-A*β* component of Alzheimer's disease amyloid; MeOH, methanol; EtOH, ethanol; PrOH, propanol; TFE, trifluoroethanol; HFiP, hexafluoro-2-propanol; TMAO, trimethylamine *N*-oxide; CD, circular dichroism; FTIR, Fourier transform infrared; ThT, thioflavin T.

10.1021/bi027166s CCC: $25.00
Published on Web 02/11/2003

recognition (*37*, *39*, *41*). In the presence of several divalent and trivalent metal ions (*43*) or several common pesticides (*44*, *45*), α-synuclein has been shown to adopt a partially folded conformation, which is critical for fibrillation. However, the binding of α-synuclein to synthetic and natural membranes is accompanied by a dramatic increase in α-helical content (*20*−*22*, *28*, *46*).

In vitro α-synuclein readily assembles into fibrils, with morphologies and staining characteristics similar to those of fibrils extracted from disease-affected brain (*30*, *47*−*56*). Fibrillation occurs via a nucleation-dependent mechanism (*49*, *54*) with the critical primary stage being formation of a partially folded intermediate (*30*). Interestingly, accelerated α-synuclein aggregation and fibrillation have also been detected as a result of the protein exposure to long chain fatty acids (*57*) and upon its interaction with lipid droplets (*27*). On the basis of these observations, it has been assumed that α-synuclein may exist in two structurally different isoforms *in vivo*: a helix-rich, membrane-bound form and a disordered, cytosolic form, with the membrane-bound α-synuclein generating nuclei that seed the aggregation of the more abundant cytosolic form (*58*).

The membrane-bound form of α-synuclein represents ∼15% of the total α-synuclein (*58*). This suggests that α-synuclein is only transiently associated with the neuronal membranes, and the majority of α-synuclein is in the non-membrane-bound form. Precedents exist for membrane surfaces modifying protein structure in cells (*59*, *60*). The negative electrostatic potential of the membrane surface can induce attraction of protons from the solution, resulting in a noticeable local decrease in pH on the membrane surface and formation of a pronounced pH gradient in its nearest surroundings (*61*, *62*). This local decrease in pH does not exceed 2 units in salt-free solutions (*62*). It is evident that such "acidification" of the local environment is insufficient for pH-induced denaturation of the majority of globular proteins, and so cannot be considered as the sole denaturing factor of the membrane surface. On the other hand, it is known from classical electrodynamics that the effective dielectric constant (ϵ) of water at the water−hydrophobic medium interface is significantly lower than in the bulk water (*63*). Such a local decrease in the dielectric constant near the membrane surface is an additional denaturing factor of the membrane (*59*, *60*).

Water/alcohol mixtures at moderately low pH values have been suggested as model systems for studying the joint action of the local decrease in pH and dielectric constant near the membrane surface on the structure of proteins (*59*, *60*, *64*−*67*).

In a quest to model the effect of membrane fields on α-synuclein, we analyzed the structural properties and aggregation and/or fibrillation propensities of this protein in mixtures of water with alcohols with aliphatic chains with different lengths (methanol, ethanol, and propanol), and fluoro alcohols (TFE and HFiP). Low concentrations of all the solvents studied induced a partially folded intermediate of α-synuclein, which strongly correlated with the propensity to fibrillate. However, protein fibrillation was completely inhibited at high solvent concentrations, with the structural effect being different for the different classes of solvents. Thus, whereas MeOH, EtOH, and PrOH induced β-rich oligomers and amorphous aggregates, TFE and HFiP induced extensive α-helical structure. Interestingly, β-rich oligomers were also observed at moderate concentrations of TFE.

MATERIALS AND METHODS

Materials

Thioflavin T was obtained from Sigma (St. Louis, MO). All other chemicals were analytical grade from Fisher Chemicals or VWR Scientific. Methanol, ethanol, propanol, 2,2,2-trifluoroethanol, and 1,1,1,3,3,3-hexafluoro-2-propanol were purchased from Aldrich. The dielectric constant values, ϵ, for water, methanol, TFE, ethanol, propanol, and HFiP were taken to be 78.3, 33.1, 27.7, 25.3, 20.8, and 16.7, respectively. In the case of a mixture of two solvents, an averaged $\langle\epsilon\rangle$ value was used, determined by the equation $\langle\epsilon\rangle = n_1\epsilon_1 + n_2\epsilon_2$, where n_i is the mole fraction of component i ($n_1 + n_2 = 1$) and ϵ_i is its dielectric constant.

Methods

Purification of α-Synuclein. Human wild-type (WT) α-synuclein was expressed in the *Escherichia coli* BL21(DE3) cell line transfected with the pRK172/α-synuclein WT plasmid (kind gift of M. Goedert, Medical Research Council, Cambridge, U.K.) and purified as previously described (*68*) with some modifications. Anion-exchange chromatography was performed on a Pharmacia AKTA FPLC system using a 5 mL High-TrapQ column. The protein was eluted with an NaCl gradient and dialyzed extensively against di-ionized water and then lyophilized in small aliquots (2 mg). Lyophilized protein was stored at −80 °C. All protein aliquots were dissolved immediately before use in 2 mM NaOH; the pH was adjusted to 11.0 with NaOH, and the protein was incubated for 10 min at room temperature (to dissolve any seeds) before the pH was readjusted to 8 with HCl. Solutions were centrifuged at 14 000 rpm for 15 min to remove large aggregates, and the supernatant was taken for the assay. The purity of the resultant protein was assessed by PAGE, gel filtration, and electrospray mass spectrometry. The protein concentration was determined by measuring the absorbance at 275 nm and using an extinction coefficient of 0.40.

Circular Dichroism (CD) Measurements. CD spectra were obtained on an AVIV 60DS spectrophotometer (Lakewood, NJ) using α-synuclein concentrations of 0.5 mg/mL. Spectra were recorded in 0.01 cm cells from 250 to 190 nm with a step size of 1.0 nm, a bandwidth of 1.5 nm, and an averaging time of 4 s. For all spectra, an average of eight scans was obtained. CD spectra of the appropriate buffers were recorded and subtracted from the protein spectra.

FTIR Spectra. Data were collected on a Thermo-Nicolet Nexus 670 FTIR spectrometer equipped with a MCT detector and an out-of-compartment germanium trapezoidal internal reflectance element (IRE). The hydrated thin films were prepared and analyzed as described previously (*69*). Typically, 256 interferograms were co-added at 1 cm^{-1} resolution. Data analysis was performed with GRAMS32 (Galactic Industries). The secondary structure content was determined from curve fitting to spectra deconvoluted using second-derivative and Fourier self-deconvolution to identify component band positions.

Analysis of Spectroscopic Data in the Form of Parametric Dependencies. The "phase diagram" method of analyzing

spectroscopic data is extremely sensitive for the detection of intermediate states (*70*−*73*). Although this method was developed for the analysis of fluorescence data, it can be used with any spectroscopic technique. The essence of this method is to build up the diagram of $I(\lambda_1)$ versus $I(\lambda_2)$, where $I(\lambda_1)$ and $I(\lambda_2)$ are the spectral intensity values measured at wavelengths λ_1 and λ_2, respectively, under different experimental conditions for a protein undergoing structural transformations (*70*−*73*).

Thioflavin T Fluorescence Assays. Assay solutions contained the protein at a concentration of 1.0 mg/mL (70 μM) in 20 mM Tris-HCl and 0.1 M NaCl (pH 7.5 at room temperature), containing 20 μM ThT with various concentrations of alcohols as indicated. A volume of 150 μL of the mixture was pipetted into a well of a 96-well plate (white plastic, clear bottom), and a $^1/_8$ in. diameter Teflon sphere (McMaster-Carr, Los Angeles, CA) was added. We have shown that the kinetics of α-synuclein fibrillation are unaffected by the presence of ThT during incubation under these conditions. Each sample was run in triplicate or quadruplicate. The plates were sealed with Mylar plate sealers (Dynex). The plate was loaded into a fluorescence plate reader (Fluoroskan Ascent) and incubated at 37 °C with shaking at 150 rpm with a shaking diameter of 20 mm. The rate of fibrillation showed some dependence on the shaking speed, and a constant shaking speed was used for all samples within each experiment. The samples were shaken to speed the rate of fibril formation. The fluorescence was measured at 15 min intervals with excitation at 450 nm and emission at 485 nm, with a sampling time of 100 ms. Data from replicate wells were averaged before plotting fluorescence versus time and fit to an empirical equation (*74*). Control experiments showed that the concentrations of alcohols used in these experiments did not significantly affect the fluorescence properties of ThT when bound to fibrils.

Dynamic and Static Light Scattering. Dynamic light scattering measurements were performed with a DynaPro instrument. Static light scattering measurements were performed in semimicro quartz cuvettes (Hellma) with a 1 cm excitation light path using a FluoroMax-3 spectrofluorometer from Instruments S.A., Inc. Jobin Yvon-Spex. Scattering profiles were recorded from 300 to 400 nm with excitation at 350 nm. For each sample, the signal was obtained as the intensity at 350 nm from which a blank measurement recorded prior to addition of α-synuclein to the solution was subtracted. All data were processed using DataMax/GRAMS software.

Electron Microscopy. Transmission electron micrographs were collected using a JEOL JEM-100B microscope operating with an accelerating voltage of 80 kV. Typical nominal magnifications were 75000×. Samples were deposited on Formavar-coated 300 mesh copper grids and negatively stained with 1% aqueous uranyl acetate.

RESULTS

Effects of Alcohols on α-Synuclein Secondary Structure

Far-UV Circular Dichroism Spectra. The effects of the simple alcohols (methanol, ethanol, and propanol) and fluoro alcohols (TFE and HFiP) on the α-synuclein structure have been compared using far-UV CD spectroscopy. Figure 1 presents far-UV CD spectra for α-synuclein solutions containing different concentrations of alcohols. Figure 1 shows that in the absence of alcohol the spectrum of α-synuclein was typical of an unfolded polypeptide chain, with a minimum in the vicinity of 196 nm, and the absence of characteristic bands in the vicinity of 210−230 nm. The addition of any of the alcohols increased the content of secondary structure manifested by a decrease in the minimum at 196 nm accompanied by an increase in negative ellipticity around 222 nm. Interestingly, the shape and intensity of far-UV CD spectra measured at low concentrations of all the solvents studied were close to those reported for the specific partially folded intermediate induced in α-synuclein by a decrease in pH or an increase in temperature (*30*), the presence of divalent and trivalent metal ions (*43*) or several common pesticides (*44*, *45*), or moderate TMAO concentrations (*75*). This partially folded intermediate conformation

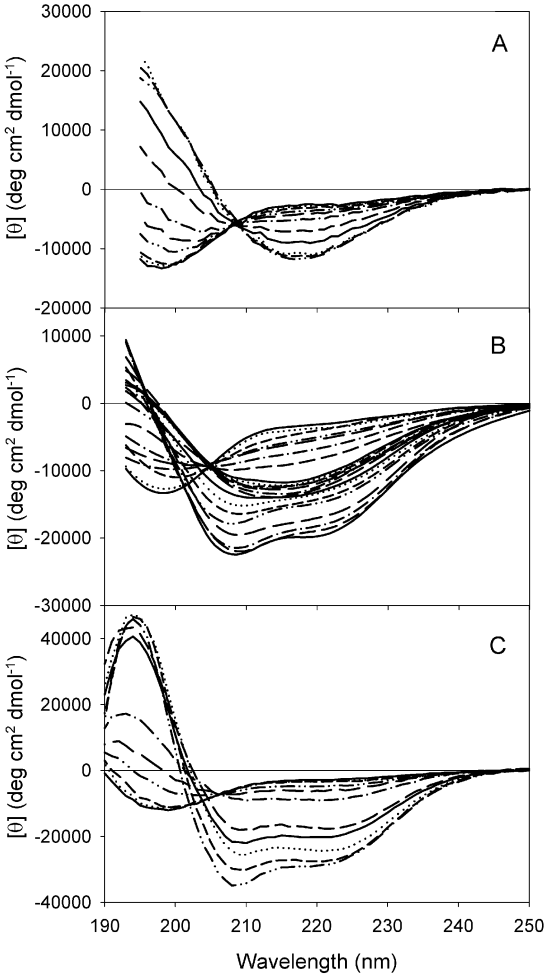

FIGURE 1: Effect of alcohols on α-synuclein conformation. Far-UV CD spectra measured for α-synuclein in the presence of increasing concentrations of different organic solvents. (A) For ethanol, the order of concentrations with increasing negative ellipticity at 220 nm is 0, 5, 10, 14, 18, 22, 28, 34, 40, 50, and 60%. (B) For TFE, the order of concentrations with increasing negative ellipticity at 220 nm is 0, 2, 5, 6, 8, 10, 11, 12, 14, 15, 16, 20, 22, 24, 25, 28, 30, 32, 35, 40, 50, and 60%. (C) For HFiP, the order of concentrations with increasing negative ellipticity at 220 nm is 0, 1, 2.0, 2.5, 3, 4, 5, 7.5, 10, 15, 20, and 40%. The data for methanol and propanol were similar to those for ethanol. Measurements were carried out at 20 °C and protein concentrations of 0.5 mg/mL.

Table 1: Oligomeric State of α-Synuclein as a Function of Alcohol Concentration and Time of Incubation[a]

	prior to incubation		after incubation for 60 h	
conditions	conformation	scattering (cps)	conformation	scattering
pH 7.5, no alcohol	unfolded	35 000 ± 3000	fibrillar	250 000 ± 5000
10% MeOH	partially folded	37 000 ± 3000	fibrillar	370 000 ± 10000
40% MeOH	β-structural	520 000 ± 10000	amorphous	2 110 000 ± 20000
5% TFE	partially folded	36 000 ± 3000	fibrillar	420 000 ± 20000
15% TFE	β-structural	410 000 ± 10000	amorphous	1 630 000 ± 20000
40% TFE	α-helical	33 000 ± 3000	α-helical	125 000 ± 7000
2.5% HFiP	partially folded	33 000 ± 3000	fibrillar	330 000 ± 10000
30% HFiP	α-helical	37 000 ± 3000	α-helical	63 000 ± 5000

[a] Static light scattering (see Experimental Procedures) was measured for selected aqueous/alcohol mixtures containing 0.5 mg/mL α-synuclein.

is associated with fibrillation. These initial structural changes observed by CD were completely reversible (data not shown) and were independent of protein concentration (at least in the range of 0.1−2.5 mg/mL; see below). This indicates that the increase in the level of structure of α-synuclein induced by low concentrations of the alcohols represents an intramolecular process and not self-association.

Subsequent structural transformations in α-synuclein at higher solvent concentrations were dependent on the type of alcohol. Thus, using ethanol as an illustrative example for the simple alcohols, higher concentrations induced a transformation of α-synuclein into a β-sheet-enriched conformation (Figure 1) based on the pronounced minimum in the vicinity of 218 nm, which is typical of folded proteins with extensive β-structure. As discussed subsequently, the β-rich species involves oligomeric forms of α-synuclein. A different situation was observed in HFiP. Figure 1C shows that for this solvent the transition started from the same partially folded intermediate but ended with formation of a helix-rich species, as shown by the two minima, at 208 and 222 nm, in the CD spectra. The latter behavior has been previously observed for a number of proteins and interpreted in terms of alcohol-induced stabilization of helical structure. A third effect of organic solvents was observed with TFE (Figure 1B). In this case, an increase in TFE concentration initially induced formation of the partially folded intermediate; then in the vicinity of 15% TFE, the β-structure-enriched species was formed, and finally, at high TFE concentrations, >35%, the α-helical conformation was observed. This species is initially monomeric but undergoes association over longer times (see Table 1).

Structural Effects of Simple Alcohols. Increasing concentrations of the three simple alcohols that were investigated induced similar changes in α-synuclein secondary structure, as illustrated in Figure 2A which represents the dependencies of $[\theta]_\lambda$ on alcohol concentration. Interestingly, the position of the transitions shifted toward lower alcohol concentrations with increased aliphatic chain length. This suggested that the driving force for the structural rearrangements of the protein might be the change in the solvent hydrophobicity.

Figure 2B, where the results are presented as the dependencies of $[\theta]_{222}$ and $[\theta]_{198}$ on the dielectric constant of the media, confirms this assumption. Using such coordinates, the structure-forming effects of different alcohols are described by a single set of "master" curves. In other words, the folding of α-synuclein in mixtures of water with simple alcohols directly correlates with the decrease in the dielectric constant of the media. Similar effects have been described

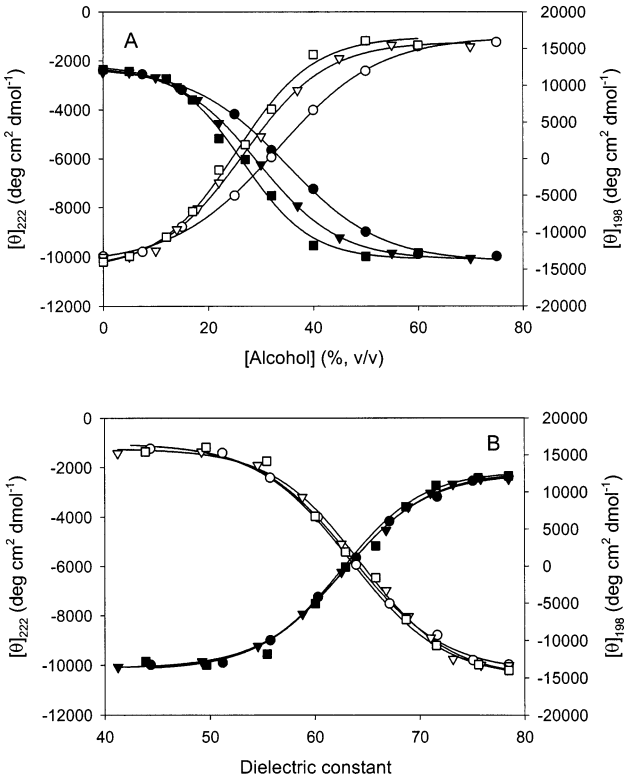

FIGURE 2: Solvent dielectric constant as the main factor determining the effect of alcohols on α-synuclein conformation. Effects of the simple alcohols [MeOH (○), EtOH (▽), and PrOH (□)] on the far-UV CD spectrum of α-synuclein. (A) Dependencies of $[\theta]_{222}$ (black symbols) and $[\theta]_{198}$ (white symbols) on alcohol concentration. (B) Dependencies of $[\theta]_{222}$ (black symbols) and $[\theta]_{198}$ (white symbols) on the dielectric constant of the media in the presence of the alcohols.

for structural transformations induced by different organic solvents in a globular protein, β-lactoglobulin (*65*, *76*).

β-Structure Formation in α-Synuclein Induced by Simple Alcohols Is Driven by Aggregation. Aggregation or self-association is a characteristic property of partially folded (denatured) proteins (*77*−*81*). It has been shown that the self-association may induce additional structure and stability in partially folded proteins (*82*−*84*), frequently an increase in β-structure content. The structural changes induced in α-synuclein by high concentrations of MeOH, EtOH, and PrOH were not reversible once the alcohols were diluted out, suggesting that association had occurred. This was confirmed by dynamic light scattering experiments. DLS analysis of the initial incubation of 0.5 mg/mL α-synuclein in 50% MeOH revealed the absence of monomer and a mixture of

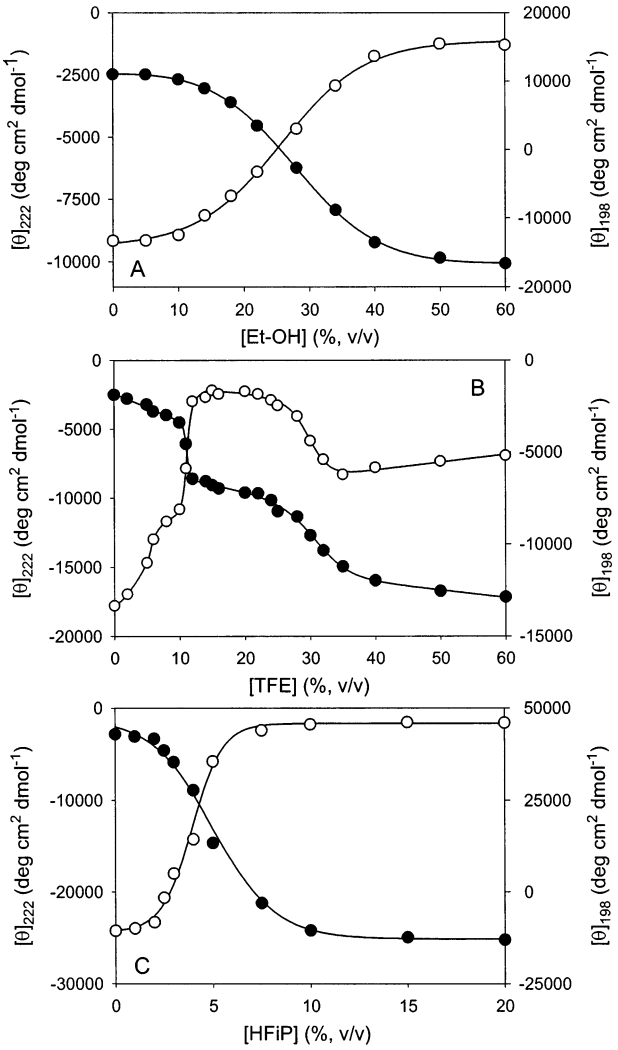

FIGURE 3: Comparison of the effects of simple alcohols with fluorinated alcohols on the conformation of α-synuclein. (A) Ethanol, as an illustrative representative for the simple alcohols, (B) TFE, and (C) HFiP. The effects of solvent concentration were measured on the α-synuclein far-UV CD spectra: $[\theta]_{222}$ (black symbols) and $[\theta]_{198}$ (white symbols). Note the different ellipticity scales.

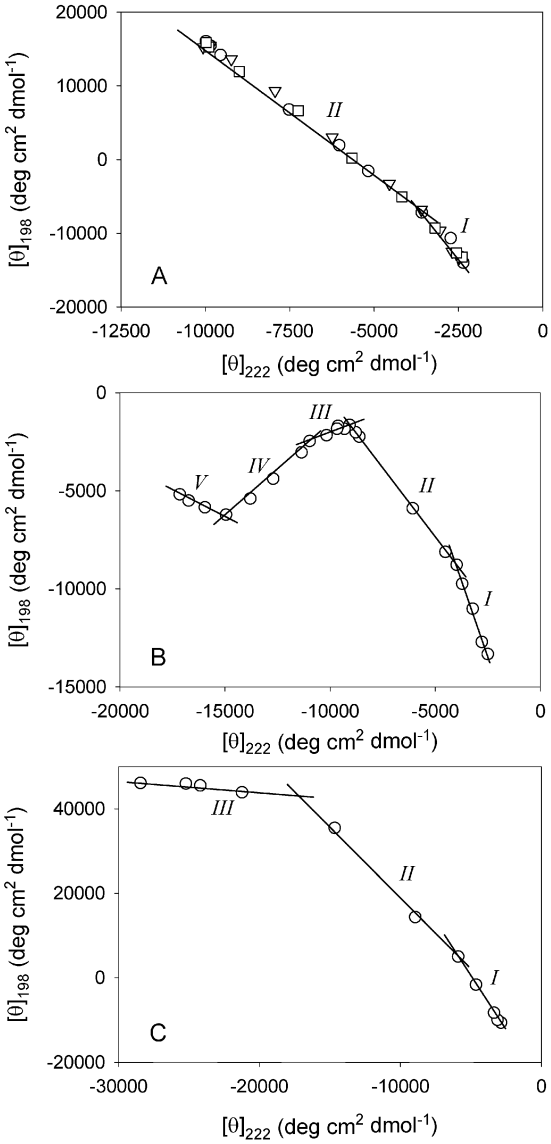

FIGURE 4: Alcohols induce multiple transitions in α-synuclein structure. Phase diagrams, based on plots of $[\theta]_{198}$ vs $\Delta[\theta]_{222}$, representing the effect of different alcohols on α-synuclein structure: (A) simple alcohols [MeOH (○), EtOH (▽), and PrOH (□)], (B) TFE, (C) HFiP. Each straight line represents an all-or-none transition between two conformers. Transitions are numbered starting from the unfolded conformation. The phase diagrams are based on the fact that the relation $I(\lambda_1) = f[I(\lambda_2)]$ will be linear if changes in the protein environment lead to an all-or-none transition between two different conformations. Thus, the nonlinearity of this function reflects the sequential character of the structural transformations, and each linear portion of the dependence describes an individual all-or-none transition. For example, panel C shows three distinct transitions.

oligomers with R_s in the range of 25−60 nm, with an average of 40 ± 10 nm. Although there was no insoluble material initially, precipitation occurred over time. Similarly, at higher protein concentrations (>3.0 mg/mL), detectable protein precipitation was observed almost immediately. Thus, in the presence of high concentrations of simple alcohols, α-synuclein underwent a conformational change and self-associated to form oligomers, which aggregated and formed insoluble (nonfibrillar) precipitates at higher protein concentrations or longer times.

Static light scattering was used to monitor α-synuclein association in the presence of the simple alcohols. The magnitude of light scattering increased significantly at higher concentrations of simple alcohols, reflecting the formation of large particles, either soluble oligomers or insoluble aggregates. At low alcohol concentrations, the initial species were monomeric; however, with increasing times of incubation, the light scattering increased, indicating self-association of α-synuclein. Some representative data from experiments with 0.5 mg/mL α-synuclein are summarized in Table 1. The results for MeOH were used to illustrate the general trends observed with the simple alcohols.

Comparison of Simple and Fluoro Alcohols. Structure-forming effects of simple and fluoro alcohols are compared in Figure 3, which illustrates the dependencies of $[\theta]_\lambda$ on the concentrations of EtOH, TFE, and HFiP. The underlying folding mechanisms of the different solvents are very distinctive. For example, panels A and C of Figure 3 show that an increase in the concentration of either EtOH (as well as other simple alcohols; see Figure 2) or HFiP is accompanied by an apparent two-state formation of folded species (to β-sheet or α-helix for EtOH and HFiP, respec-

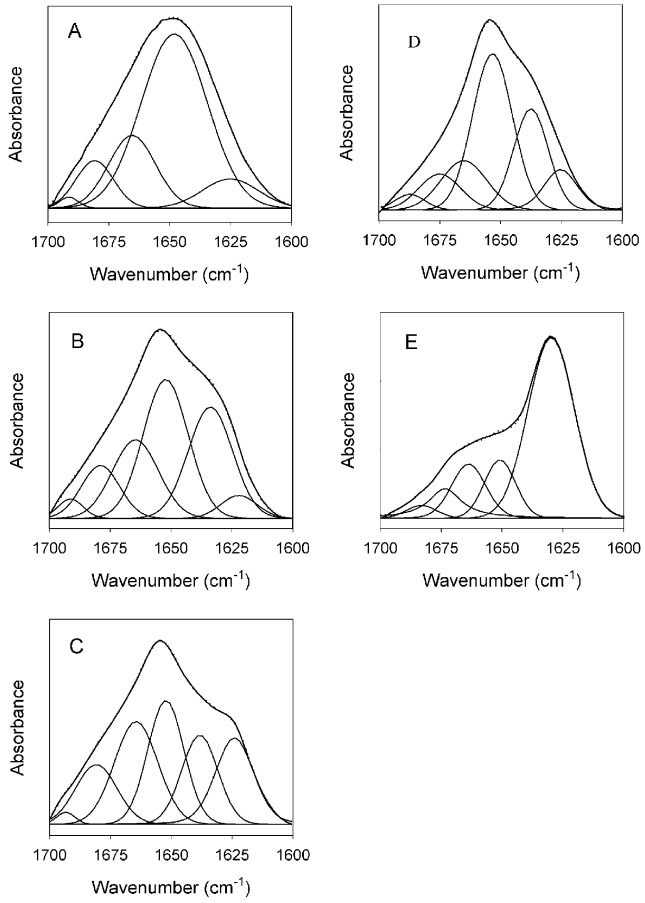

FIGURE 5: FTIR secondary structure analysis of α-synuclein in different conformational states: (A) natively unfolded (pH 7.4), (B) partially folded intermediate, induced by low concentrations of solvents, with 10% MeOH used as an illustrative example, (C) β-structure conformation induced by high concentrations of simple alcohols or moderate concentrations of TFE, with 40% MeOH used as an illustrative example, (D) α-helical form observed in high concentrations of fluoro alcohols, 20% HFiP, and (E) fibrils from aqueous buffer. FTIR spectra of the amide I region are shown as solid lines. Curve fit spectra are shown as dotted lines. Results of deconvolution (FSD and second-derivative) and curve fitting of the FTIR spectra are summarized in Table 2. Peaks in the vicinity of 1625 and 1637 cm^{-1} correspond to β-structure.

tively). The structure-forming effect of TFE is more complex and involves at least three structural transitions, separating four different conformations (see Figure 3B).

To further elucidate the mechanism of alcohol-induced conformational transformations, we have used the method of parametric dependencies or "phase diagrams". According to this method, the dependence of $[\theta]_{\lambda 1}$ versus $[\theta]_{\lambda 2}$ will be linear if changes in the protein environment lead to all-or-none transitions between two different conformations (*70*−*73*). On the other hand, nonlinearity of this function reflects multiple sequential transformations. Each linear portion of such a plot describes an individual all-or-none transition. Figure 4 represents the phase diagrams for the structural changes induced in α-synuclein by the different alcohols. Figure 4A shows that the difference in the length of the aliphatic chain did not affect the shape of the plots obtained for the simple alcohols, the phase diagrams of which were completely superimposable. These phase diagrams consisted of two linear parts, reflecting the existence of at least two independent transitions separating three different conformations (namely, the natively unfolded state, the partially folded intermediate, and the β-structure-enriched species) induced in α-synuclein by MeOH, EtOH, and PrOH.

Figure 4B shows that the structural changes induced in α-synuclein by TFE are the most complex ones, as the corresponding phase diagram has five linear parts. Some interesting information about the nature of the TFE-induced transformations of α-synuclein could be extracted from comparison of the data presented in the traditional form (Figures 1 and 3) and in the form of parametric dependencies (Figure 4). Thus, the linear regions in Figure 4 may be attributed to the following structural transitions: (I) natively unfolded → partially folded intermediate (0−10% TFE), (II) partially folded intermediate → β-structure-enriched (10−15% TFE), (III) transformations within the β-structure species (15−25% TFE), (IV) β-structure-enriched → α-helical (25−35% TFE), and (V) rearrangements within the α-helical species (35−60% TFE). As with the simple alcohols, β-structure formation induced by TFE was accompanied by protein oligomerization. The light scattering data for the effects of TFE are interesting (Table 1). α-Synuclein was initially monomeric at a low (7.5%) TFE concentration but became oligomeric by 15% TFE, and was monomeric again at high TFE concentrations (e.g., 40%). After long time periods, aggregation was observed for all TFE concentrations (Table 1).

The structural changes induced in α-synuclein by HFiP (Figure 4C) constitute three transitions: (I) natively unfolded → partially folded intermediate (0−3% HFiP), (II) partially folded intermediate → α-helical conformation (3−10% HFiP), (III) rearrangements within the α-helical species (10−20% HFiP). None of these transitions was accompanied by protein association (see Table 1).

FTIR Analysis of Organic Solvent-Induced Conformations. The data presented above are consistent with the conclusion that organic solvents may induce at least three major different conformational states in α-synuclein, a partially folded intermediate, β-structure-enriched oligomers, and monomeric α-helical species. These conformations were further characterized by FTIR. The FTIR spectrum of α-synuclein measured in the absence of organic solvent is typical of an unfolded polypeptide, whereas spectra measured under other conditions show significant changes, indicative of an increase in the level of ordered structure (Figure 5A). For example, spectra measured in the presence of low alcohol concentrations show a new shoulder in the vicinity of 1626 cm^{-1}, which corresponds to β-sheet or extended structure (Figure 5B). This means that α-synuclein contains significant amounts of β-structure in the partially folded intermediate conformation (cf. ref *30*). At high concentrations of simple alcohols (or at 15−20% TFE), the magnitude of this band further increases, reflecting subsequent enhancement of β-structure content due to oligomerization (see Figure 5C), whereas the FTIR spectra measured in the presence of high concentrations of fluoro alcohols were typical of those of α-helical proteins (Figure 5D). Finally, as expected, the FTIR spectrum of α-synuclein fibrils shows the major contribution from β-sheet (Figure 5E). Deconvolution (FSD and second-derivative) of the FTIR spectra followed by curve fitting allowed quantitation of the secondary structure in the different conformations (Table 2).

Table 2: Secondary Structure Content of Human α-Synuclein in Various Conformational States, Determined by FTIR[a]

	natively unfolded, pH 7.5		partially folded, pH 3.0		fibrils, pH 7.5	
structural assignment	wavenumber (cm^{-1})	area (%)	wavenumber (cm^{-1})	area (%)	wavenumber (cm^{-1})	area (%)
turn or β-sheet	1691	1.1	1690	1.4	1683	2.8
turn	1681	9.6	1678	5.1	1673	9.2
loops/disordered	1665	18.4	1667	17.7	1964	13.8
disordered	1649	62.1	1654	27.6	1651	13.4
β-sheet[b]			1639	22.4		
β-sheet[b]	1625	8.8	1625	25.8	1629	60.8

	partially folded, 10% MeOH		β-structure, 40% MeOH		α-helical, 20% HFiP	
structural assignment	wavenumber (cm^{-1})	area (%)	wavenumber (cm^{-1})	area (%)	wavenumber (cm^{-1})	area (%)
turn or β-sheet	1689	4.2	1693	1.2	1687	2.9
turn	1677	10.4	1680	13.4	1675	9.8
loops/disordered	1664	23.4	1664	24.4	1665	14.6
disordered	1652	29.3[c]	1652	24.4[c]		
α-helix					1653	40.7
β-sheet[b]	1635	28.2	1638	17.7	1637	22.7
β-sheet[b]	1621	4.5	1624	18.9	1625	9.3

[a] The estimated error in the frequencies is ±1.5 cm^{-1}, and ±3−5% for the areas. [b] Or the extended conformation. [c] These values could contain some contribution from α-helical structure.

Effect of Alcohols on the Fibrillogenesis of α-Synuclein

Kinetics of Fibril Formation. The histological dye thioflavin T (ThT) is widely used for the detection of amyloid fibrils (*85*−*88*). Time-dependent changes in the ThT fluorescence during the incubation of α-synuclein at 37 °C as a function of different concentrations of alcohols are shown in Figure 6. Since all the simple alcohols gave similar results, only those for ethanol are shown. The presence of the alcohols affected the kinetics of α-synuclein fibrillation in a concentration-dependent fashion. The rate of fibril formation was substantially enhanced in the presence of low concentrations of all the solvents that were studied, whereas it was completely inhibited in the solutions containing high concentrations of simple and fluorinated alcohols. The acceleration of fibril formation in the presence of low concentrations of organic solvents is due to the alcohol-induced stabilization of the partially folded α-synuclein intermediate, which was previously shown to be a critical step in the early stage of fibrillogenesis of this protein (*30*, *43*−*45*, *55*, *75*). The fact that in the presence of 40% EtOH or 20% TFE α-synuclein self-associates to form β-structure-enriched oligomers, yet does not fibrillate, suggests that these oligomers are not on the fibrillation pathway, and are quite stable. The same conclusion is also applicable for the α-helical conformation induced in α-synuclein by high concentrations of fluoro alcohols. This also may explain the lower-magnitude ThT signal observed for this protein in the presence of moderate concentrations of organic solvents (see Figure 6).

Morphology of α-Synuclein Aggregates. Fibril formation was further analyzed by electron microscopy (EM). In all experiments, we observed a strong correlation between the ThT fluorescence signal intensity and the amount of fibrils determined from EM images. EM analysis was also used to study the morphology of aggregates induced in α-synuclein by incubation in the presence of the different solvents. As illustrated in Figure 7, the overall morphology of fibrils grown in the presence of the alcohols is indistinguishable from that of fibrils grown in their absence. Furthermore, the majority of aggregated material after incubation of α-synuclein for several days under conditions stabilizing the β-sheet- and α-helix-enriched conformations was amorphous aggregate. A very few short and diffuse fibrils were also observed. This gives additional confirmation of the effective inhibition of fibrillation by the β-sheet- and α-helix-enriched conformations.

DISCUSSION

Our results demonstrate that organic solvents cause natively unfolded α-synuclein to fold in a multiphasic manner. The mechanism of such folding differed for different solvents; however, all were characterized by a common first stage leading to the formation of a previously described critical partially folded intermediate (*30*, *43*−*45*, *75*). The subsequent fate of this intermediate was dependent on the nature of the solvent (summarized in Scheme 1). Simple alcohols and moderate concentrations of TFE induced β-structure-enriched oligomers, whereas high concentrations of fluoro alcohols gave rise to an α-helical conformation. These observations mean that, depending on the environment, the partially folded intermediate may self-associate, leading to fibrils, amorphous aggregates or soluble oligomers. Furthermore, under all the conditions in which the intermediate is populated, α-synuclein fibrillates significantly faster than in control experiments. Thus, the intermediate appears to be a critical species in the fibrillation pathway.

The far-UV CD and FTIR spectra of α-synuclein in high concentrations of simple and fluorinated alcohols revealed significant ordered secondary structure. The capacity of concentrated organic solvents to induce structural changes in native globular proteins is well-established. Typically, alcohol-induced denaturation of globular proteins is accompanied by a characteristic increase in α-helix content (*64*−*67*, *76*, *77*, *89*−*97*). Much less is currently known about the behavior of natively unfolded proteins in water/organic mixtures (*98*−*100*); however, one would expect similar effects. For α-synuclein, it has been shown that solutions containing fluorinated alcohols or detergent micelles (*29*, *101*), small unilamellar vesicles (*102*), or high concentrations of TMAO (*75*) induce α-helical structure. Contrary to these observations, our data show that the effect of organic solvents

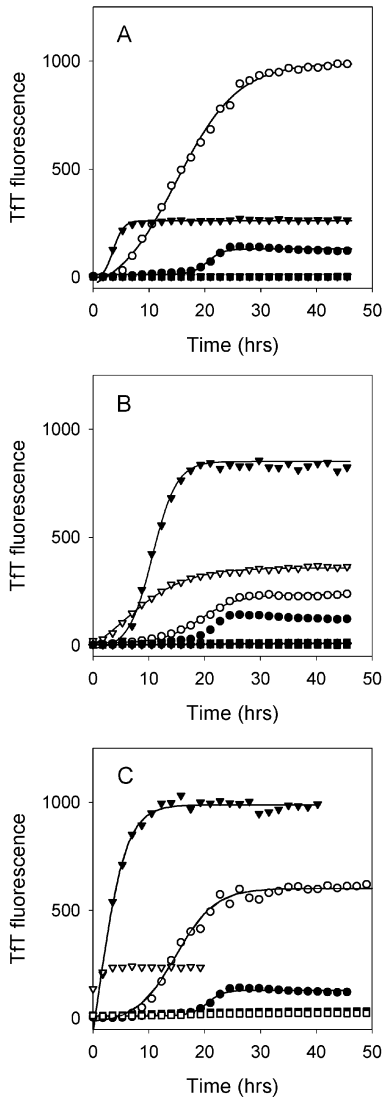

FIGURE 6: Effects of different alcohols on the fibrillation of α-synuclein. Fibrillation was monitored with thioflavin T. α-Synuclein was incubated at 37 °C with agitation in the various aqueous and organic solvents: (A) EtOH, (B) TFE, and (C) HFiP. The EtOH concentrations were 0 (●), 10 (○), 20 (▼), 25 (▽), and 50% (■) (the latter two overlap). The TFE concentrations were 0 (●), 2.5 (○), 5 (▼), 10 (▽), 15 (■), 20 (□), and 35% (⬢) (the latter three overlap). The HFiP concentrations were 0 (●), 1 (○), 2.5 (▼), 5 (▽), 20 (■), and 35% (□) (the latter two overlap). The kinetics of fibrillation were monitored by ThT fluorescence. Measurements were performed at 37 °C with agitation. The protein concentration was 1 mg/mL.

is more complex and depends on their nature and especially their concentration. In the presence of high concentrations of simple alcohols or moderate concentrations of TFE, α-synuclein forms soluble and insoluble aggregates, enriched with *β*-structure, whereas high concentrations of fluorinated alcohols induced α-helical conformation.

The structural transformations and oligomerization of α-synuclein in simple alcohols were driven by the increase in solvent hydrophobicity. In fact, the structure-forming potential of the different simple alcohols was directly proportional to the dielectric constant of the solution (Figure 2). This strongly supports the idea that the folding of α-synuclein in mixtures of water with simple alcohols is due solely to the decrease in the dielectric constant. Similarly, the structural transformations induced in a globular protein, *β*-lactoglobulin, by different alcohols have been directly attributed to the effect of the solvent polarity (*65*, *76*). These results, therefore, exclude contributions from specific protein−alcohol interactions, indicating that water/alcohol mixtures might be useful models for the effect of hydrophobic membrane surfaces (the membrane field effect) on the conformation of α-synuclein and other natively unfolded proteins. Our data are consistent with the conclusion that in the membrane field (but prior to binding to the membrane) α-synuclein first folds to the partially folded intermediate conformation and then may form either fibrils or amorphous aggregates. The effect of the membrane on protein structure will depend, in part, on the location of the protein relative to the membrane. There are three regions of importance: the hydrophobic core which is closest to the center of the membrane, followed by the interfacial region, extending slightly beyond the phospholipid headgroups into the solvent, and finally the field effect extending into the solvent. Aqueous alcohol solutions will potentially mimic the latter two regions.

Thus, on the basis of our results with the simple alcohols, we can predict that the aggregation fate of α-synuclein most probably depends on its distance from the core of the membrane: molecules localized in the proximity of the membrane, i.e., the interfacial region, will most likely form amorphous aggregates, whereas more distant molecules will be more prone to forming fibrils.

In contrast to the simple alcohols, the underlying basis for the effect of the fluorinated alcohols on α-synuclein conformation is more complex than the dielectric constant alone. This is illustrated in Figure 8 (see the discussion below) and reflects the specific interaction of the fluorinated alcohols with the protein, i.e., preferential solvation by the fluorinated alcohols. Several recent publications have shown that fluorinated alcohols preferentially bind to proteins, significantly affecting their solvation shell (*103*−*107*), whereas simple alcohols do not (*106*). In particular, it has been shown that the local concentration of TFE around bombesin (a peptide of 14 amino acid residues) was nearly twice the nominal value of the bulk concentration (*105*). We assume that this effect might be substantially greater for larger proteins, and definitely will be more pronounced for HFiP than for TFE. We assume that concentrated solutions of TFE and HFiP may be used to model the conformational changes induced in a protein due to its direct interaction with the membrane surface. Thus, the α-helical conformation induced in α-synuclein by high concentrations of TFE and HFiP most likely corresponds to the membrane surface-bound forms of this protein. It is important to note that this conformation is unable to fibrillate.

In addition, as with the simple alcohols, an increase in the concentration of fluorinated alcohols decreases the polarity of the solvent and thus can modify protein structure via the decrease in the solvent dielectric constant. This potential effect on protein structure may be enhanced at relatively low concentrations of fluoro alcohols due to their ability to preferentially solvate the protein. In Figure 8, the change in $[\theta]_{222}$ is used as a surrogate for the amount of secondary structure in α-synuclein, and is plotted against the solvent dielectric constant (black symbols). The data for TFE parallel those for the simple alcohols, but at a higher

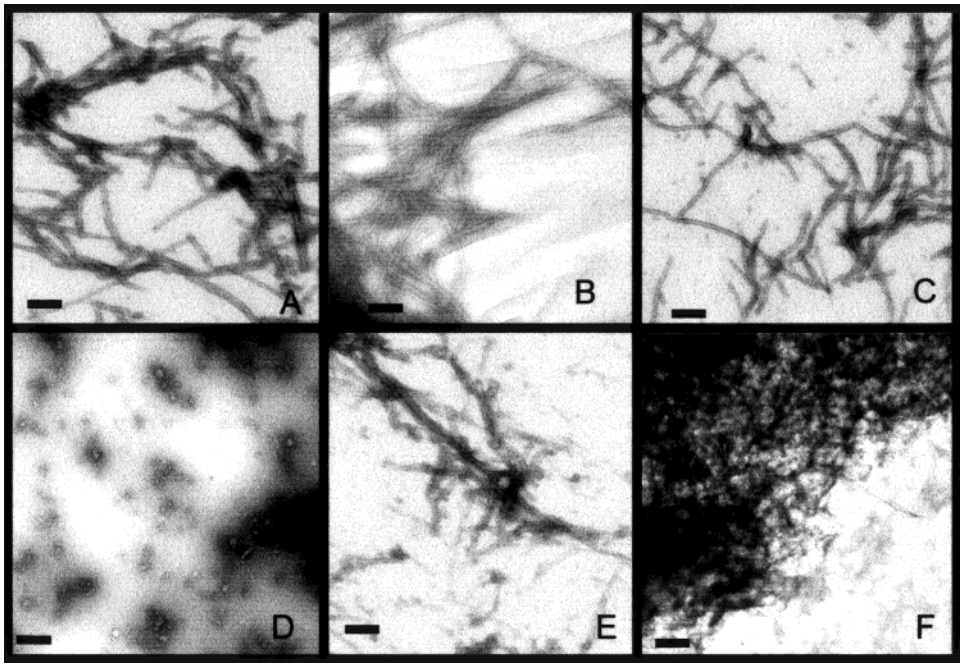

FIGURE 7: Negatively stained transmission electron micrographs of different α-synuclein aggregates induced by different alcohols. (A) Fibrils prepared from α-synuclein in the absence of organic solvents. (B) Fibrils from the partially folded intermediate induced by 10% PrOH. (C) Fibrils from the partially folded intermediate induced by 5% TFE. (D) Amorphous aggregates from 15% TFE. (E) Fibrils from 3% HFiP. (F) From amorphous aggregates from 35% PrOH. The scale bars are 100 nm in length.

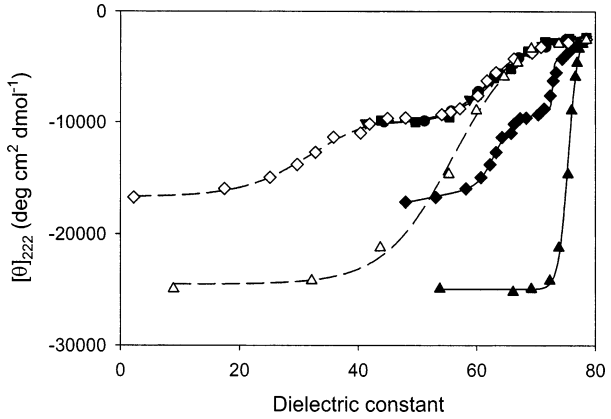

FIGURE 8: Comparison of the hydrophobic effect of simple alcohols with that of the fluorinated alcohols on α-synuclein conformational transitions. The data are displayed as $[\theta]_{222}$ vs dielectric constant: MeOH (black circles), EtOH (black inverted triangles), PrOH (black squares), TFE (gray diamonds), or HFiP (gray triangles). Data were recalculated for the preferential solvation of the fluorinated alcohols (3[TFE] or 7[HFiP]) and are shown as the white symbols (see the text). The results indicate that the transitions for the simple alcohols are solely dependent on dielectric constant, and can also account for the effect of TFE, if the effect of the local increased concentration on the dielectric constant is taken into account. However, for HFiP, additional factors are also involved.

Scheme 1

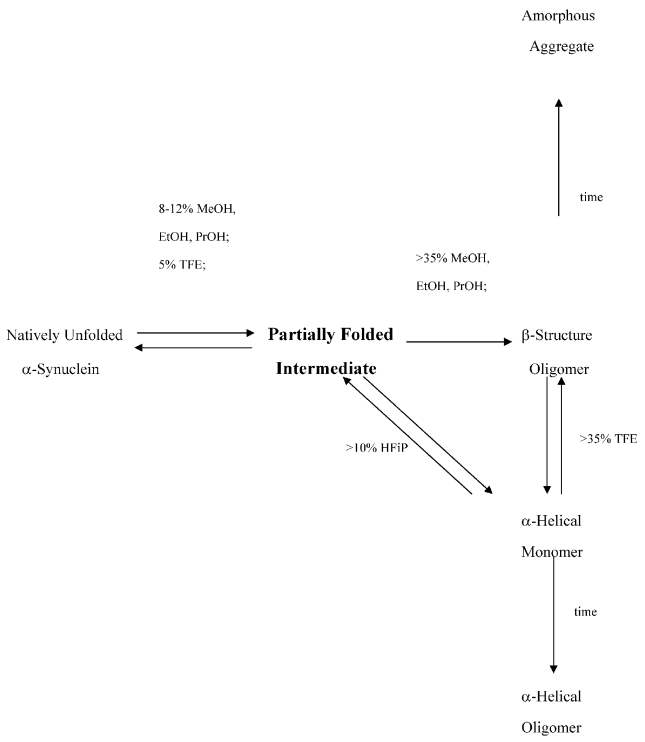

dielectric constant. Empirically, we determined that if the preferential binding of TFE results in a 3-fold greater concentration of TFE in the immediate vicinity of the α-synuclein molecules than in the bulk solvent, and that the local dielectric constant is thus correspondingly lower, then the corrected data overlap exactly those of the simple alcohols at all concentrations that were examined [Figure 8 (◇)]. Thus, a combination of preferential binding and dielectric constant effects can account for the effects of TFE. This calculation also suggests that for the simple alcohols, if the combination of chain length and concentration allowed for dielectric constants of <40, that there would be an additional transition to the helical conformation.

In the case of HFiP, the situation, as shown by Figure 8, is more complex. In fact, even if corrections are made for preferential binding of HFiP [Figure 8 (△), assuming a 7-fold increase in the local HFiP concentration], only the first part of the curve for the simple alcohols is accounted for, corresponding to the transition from the natively unfolded to the partially folded intermediate. Hence, the transition into

the α-helical conformation is distinctive and cannot be attributed just to the organic solvent-induced changes in the dielectric constant. Consequently, fluorinated alcohols have dual effects on α-synuclein and, depending on their concentration, may be used to model at least two different forms of the protein, namely, that when the protein is located in the field of the membrane (low alcohol concentrations) or that when directly interacting with the membrane, i.e., the interfacial region (high alcohol concentrations). The first form is a partially folded intermediate, which shows a high propensity to fibrillate or to form amorphous aggregates, whereas the second form is highly α-helical and is unable to form fibrils.

To explain enhanced fibrillation of α-synuclein in the presence of membranes (*27*, *57*, *58*), it has been hypothesized that *in vivo* α-synuclein may have two structurally different conformations: membrane-bound, which is enriched in α-helices, and cytosolic, which is disordered. Furthermore, it has been suggested that the membrane-bound α-synuclein may generate nuclei that seed the aggregation of the more abundant cytosolic form (*58*). Our data show that membrane-bound α-helix-enriched α-synuclein (a conformation which was effectively modeled by the high concentrations of fluorinated alcohols) most probably does not fibrillate and cannot seed the fibrils. This is supported by the observation that binding of α-synuclein to artificial membranes is accompanied by a dramatic increase in α-helical content, with coincident inhibition of fibril formation (*46*). However, our data with alcohols suggest that besides the α-helical membrane-bound form, α-synuclein may have an additional membrane-related isoform, which is induced by the membrane field, and involves the partially folded intermediate with a high propensity to fibrillate. We assume that, depending on the affinity of α-synuclein for the particular type of membrane, one of the two membrane-related forms will be predominant, giving rise to two different aggregation scenarios, a lack of fibrils in the case of the helical conformation or aggregation in the case of the partially folded intermediate. This model can account for the apparently contradictory reports of both membrane acceleration and inhibition of α-synuclein fibrillation.

REFERENCES

1. Lewy, F. H. (1912) in *Handbuch der Neurologie* (Lewandowski, M., Ed.) pp 920−933, Springer, Berlin.
2. Forno, L. S. (1996) *J. Neuropathol. Exp. Neurol. 55*, 259−272.
3. Okazaki, H., Lipkin, L. E., and Aronson, S. M. (1961) *J. Nerophathol. Exp. Neurol. 21*, 442−449.
4. Trojanowski, J. Q., Goedert, M., Iwatsubo, T., and Lee, V. M.-Y. (1998) *Cell Death Differ. 5*, 832−837.
5. Takeda, A., Mallory, M., Sundsmo, M., Honer, W., Hansen, L., and Masliah, E. (1998) *Am. J. Pathol. 152*, 367−372.
6. Lucking, C. B., and Brice, A. (2000) *Cell. Mol. Life Sci. 57*, 1894−908.
7. Spillantini, M. G., Schmidt, M. L., Lee, V. M.-Y., Trojanowski, J. Q., Jakes, R., and Goedert, M. (1997) *Nature 388*, 839−840.
8. Spillantini, M. G., Crowther, R. A., Jakes, R., Hasegawa, M., and Goedert, M. (1998) *Proc. Natl. Acad. Sci. U.S.A. 95*, 6469−6473.
9. Polymeropoulos, M. H., Lavedan, C., Leroy, E., Ide, S. E., Dehejia, A., Dutra, A., Pike, B., Root, H., Rubenstein, J., Boyer, R., Stenroos, E. S., Chandrasekharappa, S., Athanassiadou, A., Papapetropoulos, T., Johnson, W. G., Lazzarini, A. M., Duvoisin, R. C., Di Iorio, G., Golbe, L. I., and Nussbaum, R. L. (1997) *Science 276*, 2045−2047.
10. Krüger, R., Kuhn, W., Muller, T., Woitalla, D., Graeber, M., Kosel, S., Przuntek, H., Epplen, J. T., Schols, L., and Riess, O. (1998) *Nat. Genet. 18*, 106−108.
11. Masliah, E., Rockenstein, E., Veinbergs, I., Mallory, M., Hashimoto, M., Takeda, A., Sagara, Y., Sisk, A., and Mucke, L. (2000) *Science 287*, 1265−1269.
12. Feany, M. B., and Bender, W. W. (2000) *Nature 404*, 394−398.
13. Maroteaux, L., Campanelli, J. T., and Scheller, R. H. (1988) *J. Neurosci. 8*, 2804−2815.
14. Jakes, R., Spillantini, M. G., and Goedert, M. (1994) *FEBS Lett. 345*, 27−32.
15. Iwai, A., Masliah, E., Yoshimoto, M., Ge, N., Flanagan, L., de Silva, H. A., Kittel, A., and Saitoh, T. (1995) *Neuron 14*, 467−475.
16. George, J. M., Jin, H., Wood, W. S., and Clayton, D. F. (1995) *Neuron 15*, 361−372.
17. George, J. M. (2002) *Genome Biol. 3*, 3002.1−3002.6.
18. Segrest, J., De Loof, H., Dohlman, J., Brouilette, C., and Anantharamaiah, G. (1990) *Proteins: Struct., Funct., Genet. 8*, 103−117.
19. Segrest, J., Jones, M., De Loof, H., Brouilette, C., Venkatachalapathi, Y., and Anantharamaiah, G. (1992) *J. Lipid Res. 33*, 141−166.
20. Perrin, R. J., Woods, W. S., Clayton, D. F., and George, J. M. (2000) *J. Biol. Chem. 275*, 34393−34398.
21. Jo, E., McLaurin, J., Yip, C. M., George-Hyslop, P. St., and Fraser, P. E. (2000) *J. Biol. Chem. 275*, 34328−34334.
22. Volles, M. J., Lee, S. J., Rochet, J. C., Shtilerman, M. D., Ding, T. T., Kessler, J. C., and Lansbury, P. T., Jr. (2001) *Biochemistry 40*, 7812−2819.
23. Sharon, R., Goldberg, M. S., Bar-Josef, I., Betensky, R. A., Shen, J., and Selkoe, D. J. (2001) *Proc. Natl. Acad. Sci. U.S.A. 98*, 9110−9115.
24. Narayan, V., and Scarlata, S. (2001) *Biochemistry 40*, 9927−9934.
25. Volles, M. J., and Lansbury, P. T., Jr. (2002) *Biochemistry 41*, 4595−4602.
26. Ding, Y. T., Lee, S. J., Rochet, J. C., and Lansbury, P. T., Jr. (2002) *Biochemistry 41*, 10209−10217.
27. Cole, N. B., Murphy, D. D., Grider, T., Rueter, S., Brasaemle, D., and Nussbaum, R. L. (2002) *J. Biol. Chem. 277*, 6344−6352.
28. Jo, E., Fuller, N., Rand, R. P., George-Hyslop, P. St., and Fraser, P. E. (2002) *J. Mol. Biol. 315*, 799−807.
29. Weinreb, P. H., Zhen, W. G., Poon, A. W., Conway, K. A., and Lansbury, P. T., Jr. (1996) *Biochemistry 35*, 13709−13715.
30. Uversky, V. N., Li, J., and Fink, A. L. (2001) *J. Biol. Chem. 276*, 10733−10744.
31. Eliezer, D., Kutluay, E., Bussell, R., Jr., and Browne, G. (2001) *J. Mol. Biol. 307*, 1061−1073.
32. Uversky, V. N., Gillespie, J. R., and Fink, A. L. (2000) *Proteins: Struct., Funct., Genet. 42*, 415−427.
33. Uversky, V. N. (2002) *Eur. J. Biochem. 269*, 2−12.
34. Uversky, V. N. (2002) *Protein Sci. 11*, 739−756.
35. Schulz, G. E. (1979) in *Molecular Mechanism of Biological Recognition* (Balaban, M., Ed.) pp 79−94, Elsevier/North-Holland Biomedical Press, New York.
36. Pontius, B. W. (1993) *Trends Biochem. Sci. 18*, 181−186.
37. Plaxco, K. W., and Gross, M. (1997) *Nature 386*, 657−659.
38. Dunker, A. K., Obradovic, Z., Romero, P., Kissinger, C., and Villafranca, J. E. (1997) *PDB Newsletter 81*, 3−5.
39. Dunker, A. K., Lawson, J. D., Brown, C. J., Williams, R. M., Romero, P., Oh, J. S., Oldfield, C. J., Campen, A. M., Ratliff, C. M., Hipps, K. W., Ausio, J., Nissen, M. S., Reeves, R., Kang, C.-H., Kissinger, C. R., Bailey, R. W., Griswold, M. D., Chiu, W., Garber, E. C., and Obradovic, Z. (2001) *J. Mol. Graphics Modell. 19*, 26−59.
40. Dunker, A. K., Brown, C. J., Lawson, J. D., Iakoucheva, L. M., and Obradovic, Z. (2002) *Biochemistry 41*, 6573−6578.
41. Wright, P. E., and Dyson, H. J. (1999) *J. Mol. Biol. 293*, 321−331.
42. Dyson, H. J., and Wright, P. E. (2002) *Curr. Opin. Struct. Biol. 12*, 54−60.
43. Uversky, V. N., Li, J., and Fink, A. L. (2001) *J. Biol. Chem. 276*, 44284−44296.
44. Uversky, V. N., Li, J., and Fink, A. L. (2001) *FEBS Lett. 500*, 105−108.
45. Manning-Bog, A. B., McCormack, A. L., Li, J., Uversky, V. N., Fink, A. L., and Di Monte, D. A. (2002) *J. Biol. Chem. 277*, 1641−1644.

46. Zhu, M., and Fink, A. L. (2002) *J. Biol. Chem*. (submitted for publication).
47. Crowther, R. A., Jakes, R., Spillantini, M. G., and Goedert, M. (1998) *FEBS Lett. 436*, 309−312.
48. El-Agnaf, O. M. A., Jakes, R., Curran, M. D., and Wallace, A. (1998) *FEBS Lett. 440*, 67−70.
49. Wood, S. J., Wypych, J., Steavenson, S., Louis, J. C., Citron, M., and Biere, A. L. (1999) *J. Biol. Chem. 274*, 19509−19512.
50. Giasson, B. I., Uryu, K., Trojanowski, J. Q., and Lee, V. M. (1999) *J. Biol. Chem. 274*, 7619−7622.
51. Narhi, L., Wood, S. J., Steavenson, S., Jiang, Y., Wu, G. M., Anafi, D., Kaufman, S. A., Martin, F., Sitney, K., Denis, P., Louis, J. C., Wypych, J., Biere, A. L., and Citron, M. (1999) *J. Biol. Chem. 274*, 9843−9846.
52. Serpell, L. C., Berriman, J., Jakes, R., Goedert, M., and Crowther, R. A. (2000) *Proc. Natl. Acad. Sci. U.S.A. 97*, 4897−4902.
53. Conway, K. A., Harper, J. D., and Lansbury, P. T. (2000) *Biochemistry 39*, 2552−2563.
54. Conway, K. A., Lee, S. J., Rochet, J. C., Ding, T. T., Williamson, R. E., and Lansbury, P. T. (2000) *Proc. Natl. Acad. Sci. U.S.A. 97*, 571−576.
55. Li, J., Uversky, V. N., and Fink, A. L. (2001) *Biochemistry 40*, 11604−11613.
56. Hoyer, W., Antony, T., Cherny, D., Heim, G., Jovin, T. M., and Subramaniam, V. (2002) *J. Mol. Biol. 322*, 383−393.
57. Perrin, R. J., Woods, W. S., Clayton, D. F., and George, J. M. (2001) *J. Biol. Chem. 276*, 41958−41962.
58. Lee, H. J., Choi, C., and Lee, S. J. (2002) *J. Biol. Chem. 277*, 671−678.
59. Bychkova, V. E., and Ptitsyn, O. B. (1993) *Chemtracts: Biochem. Mol. Biol. 4*, 133−163.
60. Ptitsyn, O. B., Bychkova, V. E., and Uversky, V. N. (1995) *Philos. Trans. R. Soc. London, Ser. B 348*, 35−41.
61. Eisenberg, M. A., Gresalfi, T., Riccio, T., and McLaughlin, S. (1979) *Biochemistry 18*, 5213−5223.
62. Prats, M., Teissie, J., and Tocanne, J.-F. (1986) *Nature 322*, 756−758.
63. Landau, L. D., and Lifshits, E. M. (1982) *Theoretical Physics, Electrodynamics of Continuous Media*, Vol. 8, p 60, Nauka, Moscow.
64. Bychkova, V. E., Dujsekina, A. E., Klenin, S. I., Tiktopulo, E. I., Uversky, V. N., and Ptitsyn, O. B. (1996) *Biochemistry 35*, 6058−6063.
65. Uversky, V. N., Narizhneva, N. V., Kirschstein, S. O., Winter, S., and Löber, G. (1997) *Folding Des. 2*, 163−173.
66. Kamatari, Y. O., Konno, T., Kataoka, M., and Akasaka, K. (1996) *J. Mol. Biol. 259*, 512−523.
67. Narizhneva, N. V., and Uversky, V. N. (1997) *Protein Pept. Lett. 4*, 243−249.
68. Uversky, V. N., Yamin, G., Souillac, P. O., Goers, J., Glaser, C. B., and Fink, A. L. (2002) *FEBS Lett. 517*, 239−244.
69. Oberg, K. A., and Fink, A. L. (1998) *Anal. Biochem. 256*, 92−106.
70. Burstein, E. A. (1976) *Intrinsic Protein Fluorescence: Origin and Applications*, Vol. 7, VINIITI, Moscow.
71. Permyakov, E. A., Yarmolenko, V. V., Emelyanenko, V. I., Burstein, E. A., Gerday, C., and Closset, J. (1980) *Eur. J. Biochem. 109*, 307−315.
72. Bushmarina, N. A., Kuznersova, I. M., Biktashev, A. G., Turoverov, K. K., and Uversky, V. N. (2001) *ChemBioChem 2*, 813−821.
73. Kuznetsova, I. M., Stepanenko, O. V., Turoverov, K. K., Zhu, L., Zhou, J. M., Fink, A. L., and Uversky, V. N. (2002) *Biochim. Biophys. Acta 1596*, 138−155.
74. Nielsen, L., Khurana, R., Coats, A., Frokjaer, S., Brange, J., Vyas, S., Uversky, V. N., and Fink, A. L. (2001) *Biochemistry 40*, 6036−6046.
75. Uversky, V. N., Li, J., and Fink, A. L. (2001) *FEBS Lett. 509*, 31−35.
76. Dufour, E., Bertrand-Harb, C., and Haertle, T. (1993) *Biopolymers 33*, 589−598.
77. Tanford, C. (1968) *Adv. Protein Chem. 23*, 121−282.
78. DeYoung, L. R., Fink, A. L., and Dill, K. A. (1993) *Acc. Chem. Res. 26*, 614−620.
79. Fink, A. L. (1995) *Annu. Rev. Biophys. Biomol. Struct. 24*, 495−522.
80. Ptitsyn, O. B. (1995) *Adv. Protein Chem. 47*, 83−229.
81. Wetzel, R. (1996) *Cell 86*, 699−702.
82. Uversky, V. N., Segel, D. J., Doniach, S., and Fink, A. L. (1998) *Proc. Natl. Acad. Sci. U.S.A. 95*, 5480−5483.
83. Uversky, V. N., Karnoup, A. S., Khurana, R., Segel, D. J., Doniach, S., and Fink, A. L. (1999) *Protein Sci. 8*, 161−173.
84. Kuznetsova, I. M., Biktashev, A. G., Khaitlina, S. Y., Vassilenko, K. S., Turoverov, K. K., and Uversky, V. N. (1999) *Biophys. J. 77*, 2788−2800.
85. Naiki, H., Higuchi, K., Hosokawa, M., and Takeda, T. (1989) *Anal. Biochem. 177*, 244−249.
86. Naiki, H., Higuchi, K., Matsushima, K., Shimada, A., Chen, W. H., Hosokawa, M., and Takeda, T. (1990) *Lab. Invest. 62*, 768−773.
87. LeVine, H., III (1995) *Neurobiol. Aging 16*, 755−764.
88. Bartl, F., Deckers-Hebestreit, G., Altendorf, K., and Zundel, G. (1995) *Biophys. J. 68*, 104−110.
89. Tanford, C., De, P. K., and Taggart, V. G. (1960) *J. Am. Chem. Soc. 82*, 6028−6034.
90. Arakawa, T., and Goddette, D. (1985) *Arch. Biochem. Biophys. 241*, 21−32.
91. Wilkinson, K. D., and Mayer, A. N. (1986) *Arch. Biochem. Biophys. 250*, 390−399.
92. Jackson, M., and Mantsch, H. H. (1992) *Biochim. Biophys. Acta 1118*, 139−143.
93. Buck, M., Radford, S. E., and Dobson, C. M. (1993) *Biochemistry 32*, 669−678.
94. Fan, P., Bracken, C., and Baum, J. (1993) *Biochemistry 32*, 463−479.
95. Thomas, P. D., and Dill, K. A. (1993) *Protein Sci. 2*, 2050−2065.
96. Alexandrescu, A. T., Ng, Y.-L., and Dobson, C. M. (1994) *J. Mol. Biol. 235*, 587−599.
97. Hamada, D., Kuroda, Y., Tanaka, T., and Goto, Y. (1995) *J. Mol. Biol. 254*, 737−746.
98. Dahlman Wright, K., Baumann, H., McEwan, I. J., Almlöf, T., Wright, A. P., Gustafsson, J. A., and Härd, T. (1995) *Proc. Natl. Acad. Sci. U.S.A. 92*, 1699−1703.
99. Schmitz, M. L., dos Santos Silva, M. A., Altmann, H., Czisch, M., Holak, T. A., and Baeuerle, P. A. (1994) *J. Biol. Chem. 269*, 25613−25620.
100. Donaldson, L., and Capone, J. P. (1992) *J. Biol. Chem. 267*, 1411−1414.
101. Conway, K. A., Harper, J. D., and Lansbury, P. T. (1998) *Nat. Med. 4*, 1318−1320.
102. Davidson, W. S., Jonas, A., Clayton, D. F., and George, J. M. (1998) *J. Biol. Chem. 273*, 9443−9449.
103. Diaz, M. D., and Berger, S. (2001) *Magn. Reson. Chem. 39*, 369−379.
104. Gast, K., Seimer, A., Zirwer, D., and Damaschun, G. (2001) *Eur. Biophys. J. 30*, 273−283.
105. Diaz, M. D., Fioroni, M., Burger, K., and Berger, S. (2002) *Chem.—Eur. J. 8*, 1663−1669.
106. Fioroni, M., Diaz, M. D., Burger, K., and Berger, S. (2002) *J. Am. Chem. Soc. 124*, 7737−7744.
107. Roccatano, D., Colombo, G., Fioroni, M., and Mark, A. E. (2002) *Proc. Natl. Acad. Sci. U.S.A. 99*, 12179−12184.

BI027166S